J Biomol NMR (2008) 42:257–269
DOI 10.1007/s10858-008-9281-z

ARTICLE

Biosynthesis and NMR-studies of a double transmembrane domain from the Y4 receptor, a human GPCR

Chao Zou · Fred Naider · Oliver Zerbe

Received: 14 August 2008 / Accepted: 26 September 2008 / Published online: 21 October 2008

Abstract The human Y4 receptor, a class A G-protein coupled receptor (GPCR) primarily targeted by the pancreatic polypeptide (PP), is involved in a large number of physiologically important functions. This paper investigates a Y4 receptor fragment (N-TM1-TM2) comprising the N-terminal domain, the first two transmembrane (TM) helices and the first extracellular loop followed by a $(His)_6$ tag, and addresses synthetic problems encountered when recombinantly producing such fragments from GPCRs in *Escherichia coli*. Rigorous purification and usage of the optimized detergent mixture 28 mM dodecylphosphocholine (DPC)/118 mM% 1-palmitoyl-2-hydroxy-*sn*-glycero-3-[phospho-*rac*-(1-glycerol)] (LPPG) resulted in high quality TROSY spectra indicating protein conformational homogeneity. Almost complete assignment of the backbone, including all TM residue resonances was obtained. Data on internal backbone dynamics revealed a high secondary structure content for N-TM1-TM2. Secondary chemical shifts and sequential amide proton nuclear Overhauser effects defined the TM helices. Interestingly, the properties of the N-terminal domain of this large fragment are highly similar to those determined on the isolated N-terminal domain in the presence of DPC micelles.

C. Zou · O. Zerbe (✉)
Institute of Organic Chemistry, University of Zurich,
Winterthurerstrasse 190, 8057 Zurich, Switzerland
e-mail: oliver.zerbe@oci.uzh.ch

F. Naider
Department of Chemistry, College of Staten Island, CUNY,
Staten Island, NY 10314, USA

Keywords G-protein coupled receptor (GPCR) · Y receptor · Transmembrane domain · Solution NMR · Detergents

Introduction

Membrane proteins are the most abundant class of proteins in prokaryotic and eukaryotic organisms and account for 20–30% of the total genome (Boyd et al. 1998; Stevens and Arkin 2000). Amongst these, G-protein coupled receptors (GPCRs) constitute the largest membrane protein family (Foord 2002), accounting for 2% of the genome (Venter et al. 2001). GPCRs play critical roles in molecular recognition and signal transduction and are among the most pursued pharmaceutical targets (Jacoby et al. 2006). Around 30% of all marketed prescription drugs act on GPCRs, making this class of proteins a most successful therapeutic target (Hopkins and Groom 2002).

Despite their prime biological importance surprisingly little structural information is available due to the tremendous difficulties encountered in producing GPCRs in active form and the problems associated with their structural study by crystallography or NMR. Recent advances in the expression and purification of membrane proteins have been described for various expression hosts, for example: *Escherichia coli* (Drew et al. 2003, 2005; Grisshammer et al. 2005), yeast (Wedekind et al. 2006; Lee et al. 2007), insect cells (Massotte 2003), mammalian cells (Yin et al. 2005; Werner et al. 2008) and cell-free systems (Klammt et al. 2007). However, from approximately 1000 known GPCRs, only five high-resolution 3-D structures of two distinct receptor types have been reported: bovine rhodopsin (Palczewski et al. 2000) and opsin (Park et al. 2008), squid rhodopsin (Murakami and Kouyama 2008),

the human β2-adrenergic receptor (Cherezov et al. 2007; Rosenbaum et al. 2007) and the turkey β1-adrenergic receptor (Warne et al. 2008).

As long as structural studies on intact GPCRs remain complicated by technical difficulties, the study of fragments of these receptors can deliver potentially valuable insights into the structure and function of these molecules. Studies on fragments may also help to establish methods required to tackle more complex systems, in particular by providing information concerning protein-lipid interactions. While fragments of domains from soluble proteins are often not *stably* folded, in integral membrane proteins the additional stabilizing interactions that occur between TM helices and the surrounding lipids can result in stretches of the polypeptide that are conformationally defined and can be studied on their own. In 1990 Popot proposed a two-step model, the so-called partitioning-folding model, to describe assembly of membrane proteins in vivo (Popot and Engelman 1990, 2000), that was later extended by White and Wimley (1999): Initially, partitioning of the protein into the water-membrane interface results in formation of secondary structure. Interactions of the hydrophobic side chains with the surrounding lipid environment then lead to insertion of the transmembrane domains into the membrane interior. Finally, the functional protein is assembled via formation of the proper helix-helix contacts. According to this model the transmembrane domains can be thought of as independent folding units and be studied separately. A large body of literature supports the basic assumption of the model: For example, proteolysis of membrane proteins resulted in fragments containing entire TM sequences (Huang et al. 1981), and chemically or recombinantly synthesized TM peptides spontaneously assembled thereby rescuing receptor activity (Kahn and Engelman 1992; Ridge et al. 1995; Martin et al. 1999; Wrubel et al. 1994). Finally, peptides corresponding to the N and C terminus (Harmar 2001; O'Hara et al. 1993), loop domains (Bennett et al. 2004; Katragadda et al. 2001a, b; Yeagle et al. 2000) and transmembrane domains (Katragadda et al. 2001a, b; Cohen et al. 2008; Zheng et al. 2006; Musial-Siwek et al. 2008; Tian et al. 2007; Lau et al. 2008; Mobley et al. 2007; Neumoin et al. 2007) from GPCRs have been found to fold to distinct secondary structures which in certain cases resembled the structures of the corresponding regions of the intact receptor.

TM domains usually contain about 25 residues (Hessa et al. 2005, 2007), therefore double-TM constructs in phospholipid micelles should be applicable to high-resolution NMR study. Though much effort has been devoted to the study of membrane proteins both by NMR and crystallography, so far few membrane protein structures have been determined by the former technique, amongst these the F_1,F_0-ATPase (Rastogi and Girvin 1999), the bacterial mercury transport membrane protein (Howell et al. 2005) and the human glycine receptor (Ma et al. 2005), all of which comprise two TM domains. One reason why there are still so few NMR studies of larger membrane proteins published is due to the fact that sufficient quantities of labeled protein are often not available for the required trials to optimize sample conditions. In the current study we therefore tried to optimize expression of a double transmembrane fragment of the NY-4 receptor. We consider that the solutions to problems addressed in this work might be generally applicable to researchers working on polytopic membrane polypeptides.

X-ray diffraction analysis of integral membrane proteins requires high quality single crystals. In contrast NMR in solution and the solid state is independent of protein crystallization and provides complementary information to that obtained by X-ray investigations (Mackenzie et al. 1997; Getmanova et al. 2004, Klein-Seetharaman et al. 2002, 2004; Schubert et al. 2002, Oxenoid et al. 2004; Tian et al. 2005). However, NMR studies on GPCRs or large fragments of these integral membrane proteins require isotopic enrichment. This requirement makes production impossible in expression systems such as mammalian hosts, because deuteration has not been achieved to date. Moreover, membrane proteins must be studied in a membrane-like environment such as detergent micelles. The concomitant increase in molecular weight as a consequence of micelle incorporation results in a dramatic decrease in spectral quality. In addition, slow conformational exchange processes lead to additional line-broadening. This has led to the frequently encountered experience that signals from the TM regions of membrane proteins remain invisible (Tian et al. 2005). The lack of availability of fully deuterated detergents, compounds the technical difficulty of obtaining high resolution spectra for GPCRs or their fragments in micelles.

Herein, we report on the expression and purification of a 115-residue (121 residues with the His tag) fragment from the neuropeptide Y4 GPCR containing the N terminus, the first transmembrane domain (T1), the first intracellular loop (I1), the second transmembrane domain (T2), and the first extracellular loop (E1) followed by a $(His)_6$ tag. This peptide (N-TM1-TM2) comprises about one third of the total length of the receptor (Fig. 1) and was obtained in multimilligram quantities. Importantly, the construct contains no fusion that needs to be removed after expression, and hence bypasses problems associated with chemical cleavage in the presence of residues like Met, or the enzymatic cleavage of hydrophobic sequences in the presence of detergents. Spectra with good quality could only be obtained when working under reducing conditions which eliminated fragment oligomerization. Detergent mixtures proved to be necessary to yield the high quality

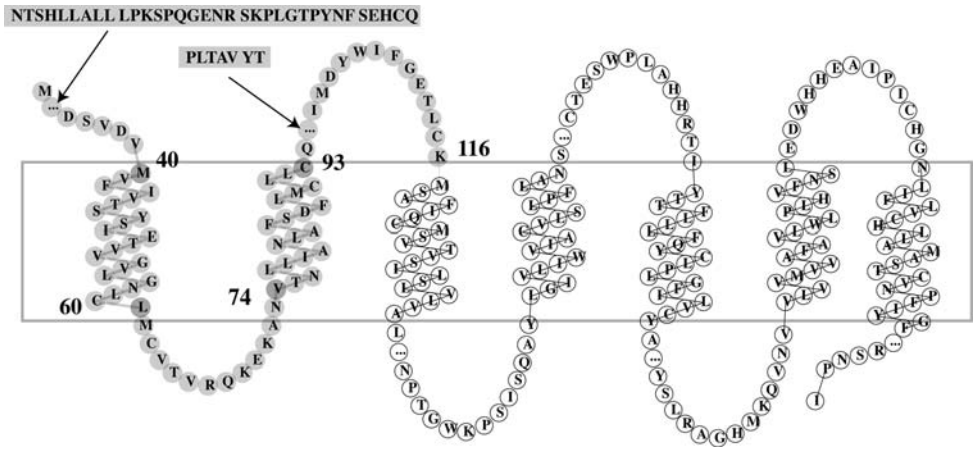

Fig. 1 "Snake"-plot type presentation of the human Y4 receptor. The plot was modified from a download from the GPCR.org website. The part of the receptor that has been expressed in this work is shaded in gray. Note that the expressed polypeptide additionally contains a C-terminal $(His)_6$ tag. The omitted sequences for parts of the N terminus and the E1 loop are indicated separately in the figure

spectra required for our analyses. Using a 1-palmitoyl-2-hydroxy-*sn*-glycero-3-[phospho-*rac*-(1-glycerol)] (LPPG)/dodecyl-phosphocholine (DPC) mixture and uniform ^{2}H,^{13}C,^{15}N labeling, TROSY-based 3D triple-resonance spectra could be recorded that allowed almost complete assignment of the backbone nuclei. The secondary chemical shifts indicate that the peptide is largely helical except for a mostly unfolded N-terminal domain.

Materials and methods

Plasmid construction

The forward primer CGCGCT**CATATG**ATGAACACCT CTCACCTCCTG, in which bold letters denote a NdeI cleavage site and the backward primer AGCGCG**GGAT CC***TCA*GTGATGGTGATGGTGATGCTTGCAGAGGGT CTCTCCAAA, in which bold letters denote a BamHI cleavage site, italic letters the stop codon and underlined letters the 6× His tag, were used to amplify the gene encoding N-TM1-TM2 from the cDNA of the Y4 receptor (University of Missouri-Rolla, USA). The amplified gene was ligated into the plasmid pLC01 after both were cleaved with *Nde*I and *Bam*HI and purified from agarose gel. The correctness of the recombinant DNA was confirmed by dideoxy sequencing (Synergene Biotech, Switzerland).

Protein expression and purification

The plasmid encoding the target protein was transformed into BL21-AI cells for expression, which were previously shown to result in higher expression levels compared to other strains (Cohen et al. 2008). A freshly transformed colony was used to inoculate 10 ml LB containing 100 mg/ml ampicillin. This preculture was grown over night at 37°C and was then used to inoculate 1L LB (for the unlabeled sample) or M9 (with $^{15}NH_4Cl$ and ^{13}C glucose as sole nitrogen and carbon sources) media containing 100 mg/ml ampicillin and cultured at 37°C until the OD_{600} reached 0.45–0.5. For induction the temperature was lowered to 20°C and 0.2% L-arabinose was added. Cells were harvested after 12 h and stored at −20°C until further use. To allow expression in deuterated water transformed BL21-AI cells were plated on a D_2O M9 agar plate, and one colony was used to inoculate a LB preculture in 100% D_2O containing 100 mg/ml ampicillin. The preculture was grown at 37°C overnight and was then used to inoculate 1 l 95% D_2O M9 containing 75 μg/ml ampicillin. After incubation at 37°C overexpression was induced when the OD_{600} had reached 0.45 by adding 0.2% L-arabinose at 20°C, and cells were harvested after 24 h.

The cell pellet from 1 L culture was resuspended in GdHCl-containing buffer and the target protein purified from inclusion bodies under denaturing conditions using Ni-affinity chromatography. The protein was incubated together with 100 mM DTT, 250 mM mercaptoethanol, 10 mM EDTA at 4°C over night to reduce any disulfide bonds. The reduced eluant was purified by C4 reverse-phase HPLC using a H_2O/acetonitrile solvent system containing 0.1% TFA. The correctness of the target peptide was confirmed by MALDI-TOF (in case of unlabeled sample: 13645, theoretical mass: 13647.9) as well as western blotting with anti-His antibody and N-terminal amino acid sequencing. The level of deuteration for the sample that was used for the backbone assignment was approx. 65% according to MS. Incomplete deuteration is solely due to back-exchange from labile protons and protons picked up from the non-deuterated glucose.

NMR sample preparation

1.7 mg ^{15}N or ^{2}H,^{13}C,^{15}N uniformly labeled protein was dissolved in 200 μl 90% H_2O/D_2O containing 2.5 mg DPC by thorough sonication and shaking at 37°C for 30 min.

15 mg LPPG were dissolved in 50 µl 0.2 mM phosphate buffer (pH 6.0), after which the two detergent solutions were mixed. The final concentration for each component in the final solution was as follows: 0.5 mM protein, 1% (28 mM) DPC, 6% (118 mM) LPPG, 10% D_2O and 40 mM phosphate buffer (pH 6.0). The sample was stable for more than 2 months at 4°C and more than 2 weeks at 47°C.

NMR spectroscopy and backbone assignment

All data were recorded on Avance 600 and 700 MHz Bruker spectrometers using triple-resonance cryoprobes at 47°C. Chemical shifts of protons were calibrated according to the water line at 4.53 ppm at 47°C, from which the carbon and nitrogen chemical shifts were referenced indirectly using the conversions factors published on the BMRB database. Sample optimization was conducted using solely ^{15}N-labeled samples and [^{15}N,^{1}H]-TROSY spectroscopy (Pervushin et al. 1997). For backbone assignments standard Bruker experiments for the TROSY versions (Salzmann et al. 1998, 1999) of the 3D HNCACB (Shan et al. 1996; Wittekind and Mueller 1993), HN(CO)CACB (Shan et al. 1996), HNCO (Yamazaki et al. 1994) and HN(CA)CO (Yamazaki et al. 1994) and a 200 ms ^{15}N-NOESY were used. For the HNCACB or HN(CO)CACB experiments 1024(^{1}H)*20(^{15}N)*80(^{13}C), for the HNCO or HN(CA)CO experiments 1024(^{1}H)*20(^{15}N)*32(^{13}C), and for the 3D ^{15}N-resolved NOESY 1024(^{1}H)*20(^{15}N)*125(^{1}H) complex data points were acquired. Spectral widths (and carrier positions) were 26 ppm (118.0 ppm) for ^{15}N, 60 ppm for ^{13}C in the experiments that label Cα and Cβ resonances with the carbon carrier at 39 ppm for Cαβ and 54 ppm for Cα. In the HNCO-type experiments 20 ppm were used for carbon, with the carrier set to 176 ppm. All experiments used pulsed field gradients for water suppression (Keeler et al. 1994), and the Kay-Palmer sensitivity enhancement trick (Kay et al. 1992) as incorporated into the TROSY sequences by Weigelt (Weigelt 1998). A proton-detected version of the steady-state ^{15}N{^{1}H} heteronuclear Overhauser effect sequence was used for measurement of the heteronuclear NOE using a train of 120° proton pulses separated by 5 ms over a period of 3 s to achieve saturation of amide protons (Noggle and Schirmer 1971). ^{15}N{^{1}H}-NOEs were computed from the ratio of integrals from signals in the presence to those in the absence of amide proton irradiation.

Spectra were processed within the Bruker spectrometer software Topspin 2.0. Backbone assignment was accomplished within the software CARA (Keller 2004). Preferences for secondary structure based on ^{13}Cα, ^{13}Cβ, ^{13}CO and ^{15}N chemical shifts were computed with the program TALOS (Cornilescu et al. 1999).

Circular dichroism spectroscopy

CD spectra were recorded on Jasco model J-810 using 50 µM protein in 40 mM phosphate buffer (pH 6.0) in a mixture of 1% DPC and 6% LPPG in a quartz cuvette with a path length of 1 mm. All spectra were averaged from 3 consecutive measurements in the range between 190 and 250 nm at 47°C with a slit width of 1 nm and a scanning rate of 5 nm/min. The blank sample was recorded under identical conditions and subtracted from the sample spectra. The final CD intensity is expressed as the mean residue ellipticity (deg cm^2 dmol^{-1}).

Results

Optimization of protein expression

In order to obtain maximum expression of N-TM1-TM2 four different strains, BL21(DE3), C41(DE3) (Miroux and Walker 1996), BL21-AI and BL21-pLys(DE3), were evaluated. Amongst these BL21(DE3) is the most widely used expression host, while the other strains have been developed to express toxic proteins. Expression was tested for each strain at 37°C and 20°C. As shown in Fig. 2 temperature has a dramatic effect on the expression level of the target protein, which is significantly higher at 20°C than at 37°C. Although BL21(DE3) expresses the target protein at 20°C, the reduced levels in comparison to the other strains that we tested indicates that the target protein may be toxic to this strain. Considering the perfect control of leakage expression, BL21-AI was chosen as the host for large-scale expression; nevertheless the difference in comparison to strains C41 or BL21pLys(DE3) is small.

The chosen construct comprises six cysteine residues, some of which will spontaneously form disulfide bonds, in particular in the presence of the divalent cation Ni^{2+}. Protein preparations in both reducing and non-reducing sample buffer were analyzed by SDS-PAGE. It was observed that dimers, trimers and other oligomeric forms are observed in the non-reducing sample. Furthermore, we noticed the presence of a smear in the gel suggesting the occurrence of non-specific aggregation. Upon addition of 100 mM DTT to the sample buffer the smearing disappeared and the oligomerization was dramatically reduced indicating that disulfide bond formation was responsible for aggregation.

Optimization of purification and detergent

The protein recovered after Ni affinity chromatography and treatment with DTT was fairly homogeneous as judged by

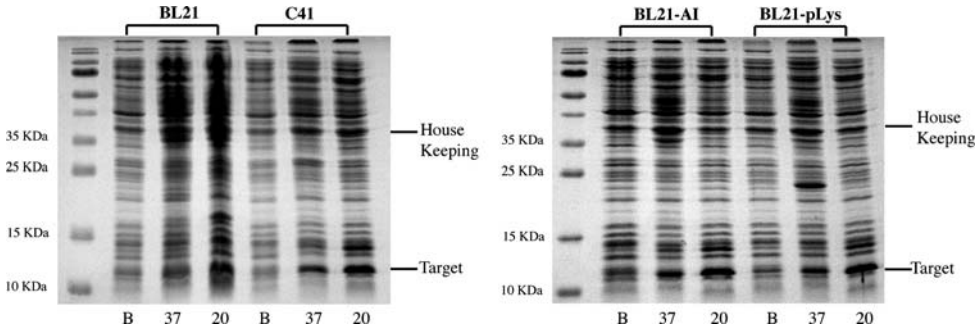

Fig. 2 Selection of strain and expression conditions shown for BL21 and C41 (left) and for BL21-AI and BL21 pLys (right). B denotes "before induction", 37 denotes "induction at 37°C" and 20 denotes "induction at 20°C"

SDS-PAGE. Nevertheless, the [^{15}N,^{1}H]-TROSY spectrum still displayed too few peaks, and peak intensities varied considerably. The latter characteristic is most likely due to conformational exchange processes. We reasoned that lipid components from the cell membrane or other hydrophobic impurities that co-elute with N-TM1-TM2 from the affinity column may result in a conformationally heterogeneous interaction/integration into the phospholipid micelles. Using this protein preparation we were unable to identify detergents that resulted in better spectra (*vide infra*). Accordingly the eluant from the Ni affinity column was subjected to C4 reverse-phase HPLC. The detrimental effects on spectral quality of contaminants remaining after Ni affinity chromatography have also been recently discussed by Page et al. (2006). The overall yield from a 1 l M9 culture of transformed BL-21AI cells after this additional step of chromatography was approximately 6 mg. We also noticed to our surprise that after lyophilization the solubility of the HPLC-purified protein in certain detergents had completely changed.

In order to obtain resolved TROSY spectra with sharp peaks a number of detergents were screened, including anionic (SDS, sarcosyl, LPPG, LMPG), zwitterionic (DPC, DHPC, LDAO) and non-ionic (OGP, DDM) detergents, and proton-nitrogen correlation spectroscopy was used to assess the suitability of the resulting samples for structural studies. As shown in Fig. 3 different detergents resulted in vastly different spectra. In some detergents tested the target protein was insoluble. Spectra measured in most detergents that dissolved the protein were of poor quality in that most of the expected peaks were missing and that some lines were very broad (Fig. 3g, h). Spectra recorded in the presence of SDS micelles resulted in too many peaks albeit that they were very sharp (Fig. 3f). In addition, measurements of the ^{15}N{^{1}H}-NOE indicated that the protein was highly flexible.

While the protein after elution from the Ni affinity column was nicely soluble in 200 mM LPPG solution, it turned out to be largely insoluble in the same detergent after the additional HPLC step. In contrast, it was now well soluble in DPC solution, a detergent in which the eluant from the Ni-affinity column was insoluble. Since it was observed that low-concentration samples prepared in LPPG resulted in good spectra, and considering the fact that DPC can solublize the protein well, we tested mixtures of these two detergents to exploit the individual advantages of both. First the minimal concentration of DPC required to dissolve at least 0.5 mM protein was determined. Then increasing amounts of LPPG were added to DPC until a good-quality spectrum was obtained, and no further chemical shift changes upon addition of more LPPG occurred. The final detergent mixture consisted of 6% LPPG and 1% DPC and was used in all subsequent studies. The TROSY spectra recorded on such a sample displayed rather uniform linewidths. In addition, the ^{15}N{^{1}H}-NOE data indicated that the backbone is rather rigid and that secondary structures are likely formed (see Fig. 6). Estimation of the overall correlation time derived from the ^{15}N R2/R1 ratio resulted in a value of 11.4 ns at 47°C.

Spectroscopy and backbone assignment

Considering the rather large molecular weight of the N-TM1-TM2/DPC/LPPG mixed micelle deuteration of the peptide was essential to yield spectra of sufficient quality. For backbone assignment a threefold strategy was pursued: (i) matching of amide moieties via common C$\alpha\beta$ resonances in the HNCACB and HN(CO)CACB experiment, (ii) matching via common CO frequencies in the HNCO and HN(CA)CO experiments, and (iii) NOEs between sequential amide protons. Approx. 70% deuteration and the comparably narrow amide lines allowed for efficient TROSY-type triple resonance experiments. Alpha helical transmembrane proteins have intrinsically less signal dispersion and only constant-time ^{13}C and ^{15}N evolution in combination with mirror-image linear prediction provided sufficient resolution. Correlations in the triple-resonance HNCA and HNCACB spectra were observed for more than 80% of all residues. In the HNCO/HN(CA)CO pair correlations were almost always present. Representative strips from the assignment process are depicted in Fig. 4. Matching strips could be confirmed in the ^{15}N-resolved NOESY for all residues within the helical region with sufficient resolution in the proton frequency. In the end all

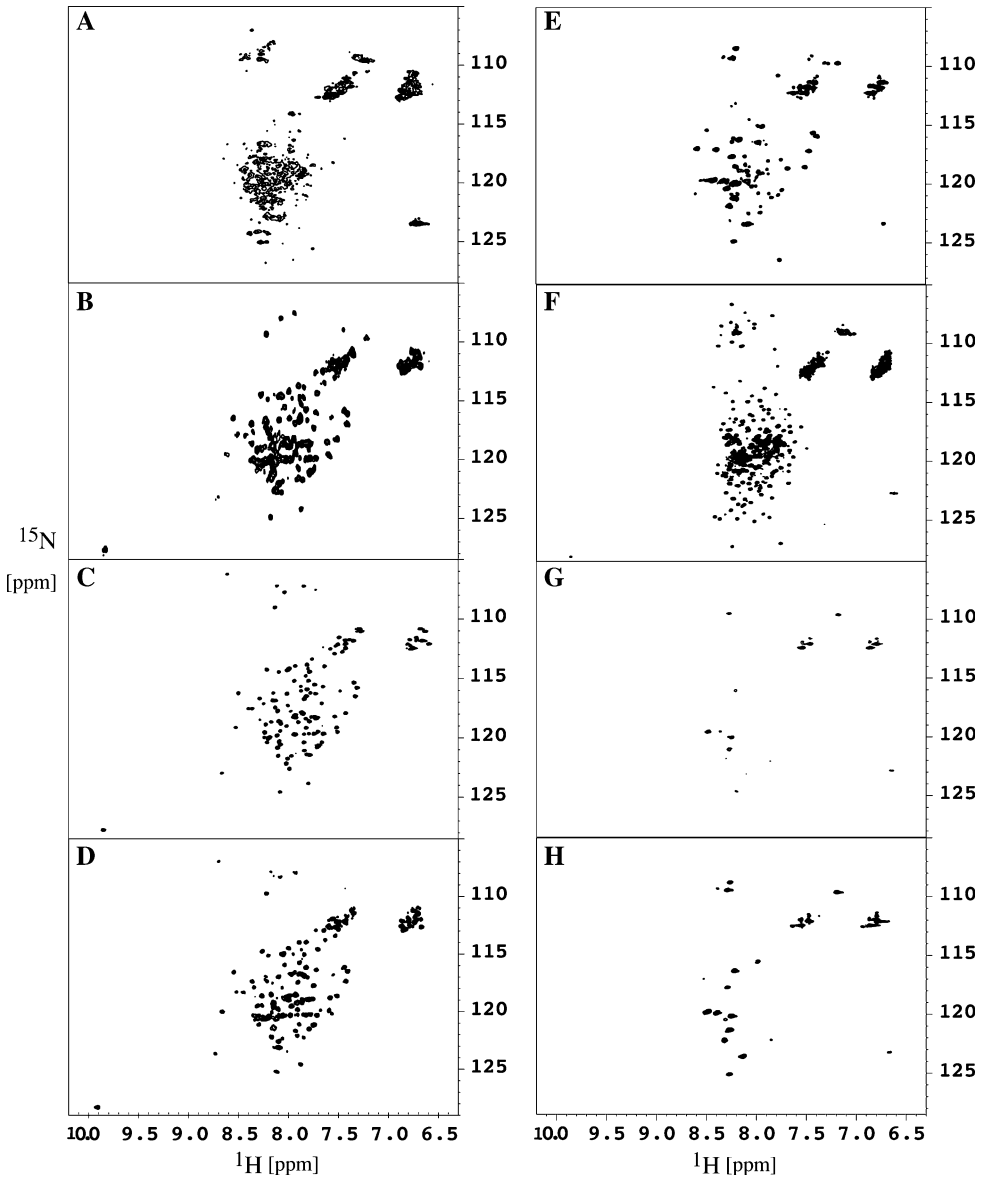

Fig. 3 Plots of the two-dimensional [^{15}N,^{1}H]-HSQC spectra of N-TM1-TM2 recorded on samples of varying degrees of purity (spectra A–D) in various detergents (spectra E–H). Spectra were recorded using 0.3 mM samples of the protein at pH 6.0 in 200 mM LPPG (**a**, **b**, **d**), 30 mM DPC/100 mM LPPG (**c**), 150 mM DPC (**e**), 170 mM SDS (**f**), 170 mM OGP (**g**) and 100 mM DHPC (**h**) at pH 6.0. The spectra on the left display protein samples directly after the Ni-affinity chromatography (**a**), after additional reduction with 100 mM DTT and 250 mM mercaptoethanol (**b**), after additional RP-HLPC in LPPG/DPC (**c**) and after purification and refolding using a method proposed by Page et al. (2006) (**d**). The spectra on right were recorded with protein samples of highest purity and homogeneity. All data were recorded at 47°C at 700 MHz proton frequency and the recognizable peak numbers out of the expected 115 are 74 (**b**), 109 (**c**), 97 (**d**), 63 (**e**), 161 (**f**), 12 (**g**), 15 (**h**), respectively, and is impossible to determine in (**a**)

H^N, N, Cα and Cβ nuclei could be assigned except for residues number 2 and 5, which are located in the flexible N terminal domain. Chemical shifts have been deposited in the BMRB database under accession code 15921.

Secondary structure

The CD spectrum of N-TM1-TM2 in DPC/LPPG mixed micelles is depicted in Fig. 5. For technical reasons, 50 μM polypeptide was used in comparison to 0.5 mM in the NMR sample. However based on the NMR spectra no aggregation occurred at the higher concentration and we believe the data obtained from the CD and NMR study are comparable. The CD spectrum clearly shows the presence of minima at 208 and 222 nm, typical for predominantly alpha helical conformations. In addition, deconvolution of the CD spectrum into contributions from the different secondary structural elements using the program K2D (http://www.embl-heidelberg.de/~andrade/k2d/) allowed estimating the content in α-helix to be around 57%. The CD analysis indicates that secondary structure under these conditions is properly formed.

In order to verify the results from the CD analysis, we have evaluated the ^{15}N{^{1}H}-NOE to derive information on the rigidity at residue resolution. The data are depicted in Fig. 6 and compared to structural and dynamical properties of the isolated N-terminal domain from the Y4 receptor recently determined by us in the presence of pure DPC micelles at pH 5.6 (Zou et al. 2008). The latter structural studies revealed the presence of a short α-helical stretch comprising residues 5–10, followed by a longer flexible loop in the segment between residues 11 and 25.

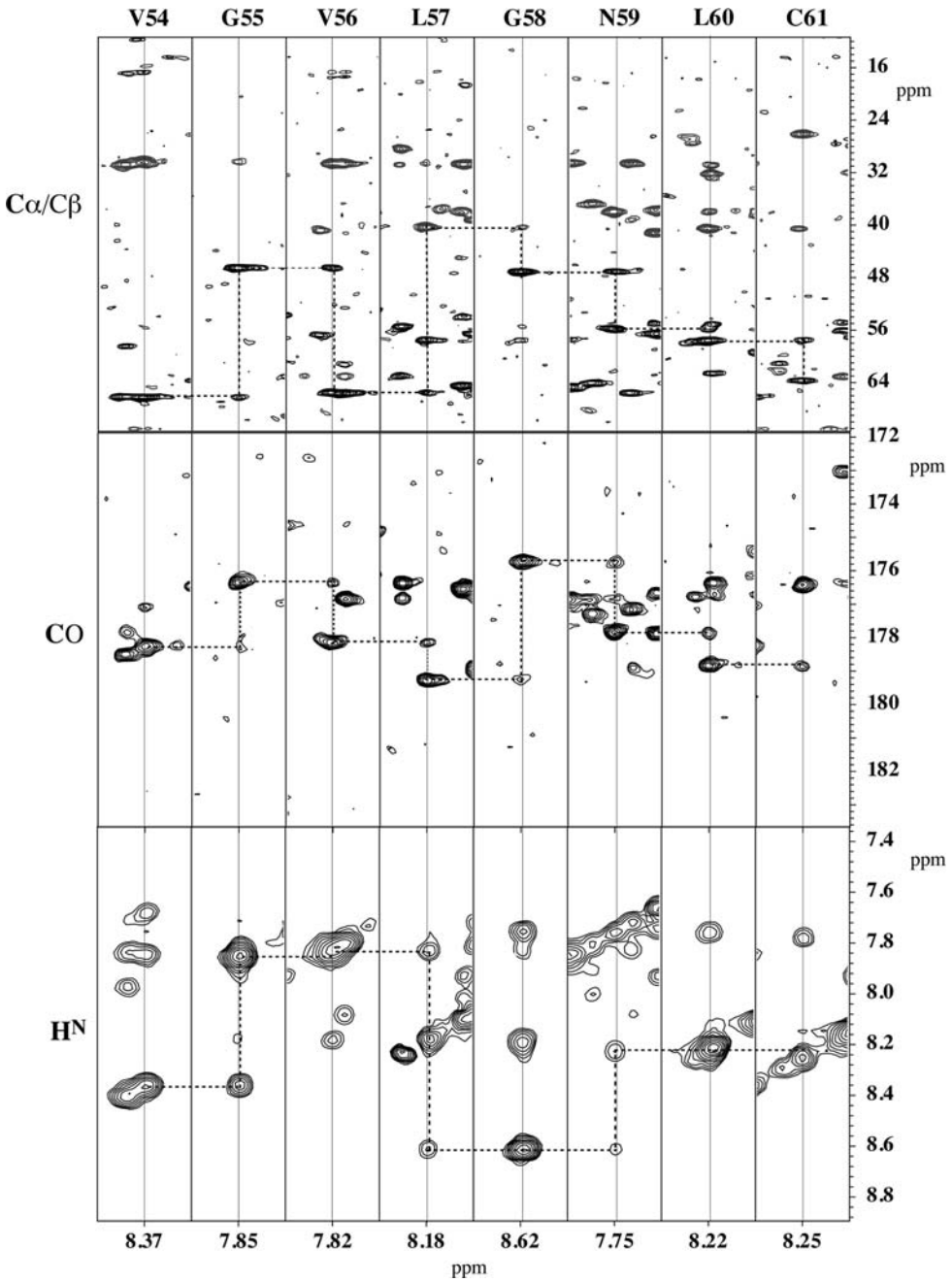

Fig. 4 Plot displaying strips from the HNCACB (top), the HN(CA)CO (middle) and ^{15}N-NOESY spectra for the TM segment comprising residues Val54 to Cys61. Only Cα resonances are connected in the top panel. Strips were extracted at the ^{15}N chemical shifts of the corresponding amide nitrogen. All data were recorded at 700 MHz at 47°C using the ^{2}H,^{13}C,^{15}N triply labeled protein in the 28 mM DPC/ 118 mM LPPG detergent mixture in 40 mM phosphate buffer, pH 6.0

Interestingly, the data on the construct described in this work indicated the presence of this flexible loop even when the N-terminal domain was fused to the first two helices. Otherwise the data indicate that with the exception of the N-terminal domain the protein is highly structured. Surprisingly, little difference in rigidity is observed between residues from the putative TM helices and the loops. In addition the long first extracellular loop (E1), that in our construct lacks its native connection to the third TM, is rather rigid. Amide hydrogen exchange as measured in a [^{15}N,^{1}H]-HSQC experiment with and without presaturation of the water resonance revealed accelerated exchange only for the N-terminus, for the long unstructured loop in the N-terminal domain (data not shown) and in vicinity to the charged residue within TM1. Surprisingly, even in the I1 or E1 loop, hydrogen exchange is relatively slow indicating that these segments are reasonably folded and/or protected from solvent access.

Sidechain assignment is presently in progress, which will help establishing secondary structure based on characteristic medium-range NOEs. However, backbone ^{15}N, Cα, Cβ and C$'$ shifts have already been assigned and hence the location and type of secondary structure can be predicted based on secondary chemical shifts (Wishart and

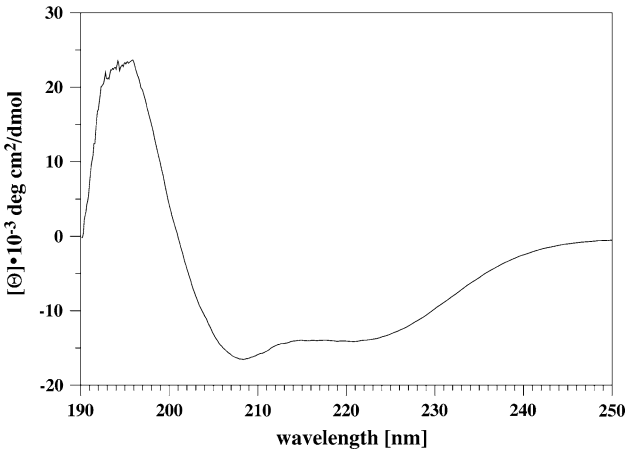

Fig. 5 CD spectrum of 50 μM N-TM1-TM2 recorded at 47°C in 40 mM phosphate buffer (pH 6.0) containing a mixture of 28 mM DPC and 118 mM LPPG. Data are converted to mean residue ellipticity

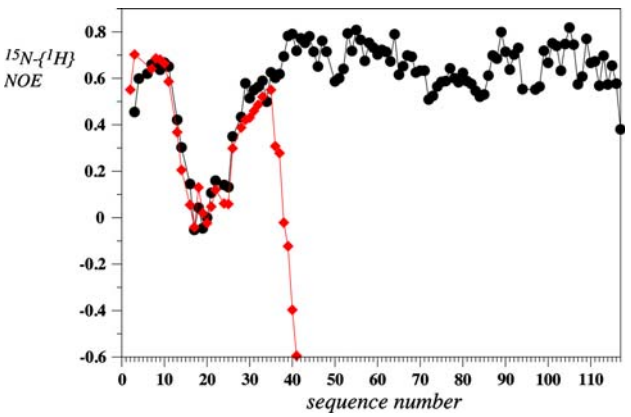

Fig. 6 Comparison of the $^{15}N\{^{1}H\}$-NOE values for N-TM1-TM2 (black spheres) described in this work and the isolated N-terminal domain from the Y4 receptor (N-Y4, red diamonds). All values were measured on the 600 MHz spectrometer. Data of N-Y4 are taken from Zou et al. (2008)

Sykes 1994; Wishart et al. 1991). The output of the program TALOS (Cornilescu et al. 1999) is depicted in Fig. 7. It predicts 74% of the 77 residue C-terminal fragment (the 2 TM helices plus the loops) to be helical. Interestingly, in both TM helices TALOS predictions indicate the TM helices to be destabilized adjacent to the internal polar residues Glu51 and Thr52 in TM1 or Ser86 and Asp87 in TM2. Accordingly, no predictions were made for these regions. The locations of helical segments were also probed using proton,proton NOEs. In helices comparably short distances occur between sequential amide protons. Figure 4 shows contacts within the segment encompassing residues Val54–Cys61 that are consistent with such short distances. Comparably strong NOEs between sequential amide protons occur through most of the residues in the TM1/TM2 segments. Additionally they are observed for most of the residues from the I1 and E1 loops.

Discussion

Considering the tremendous difficulties encountered during expression, purification, reconstitution and the spectroscopic evaluation of entire GPCRs, new strategies to derive useful structural information are highly desired. Accordingly, in this work we developed synthetic approaches for a double-TM construct that additionally contains the N-terminal domain and the first extracellular loop.

To our knowledge despite the success reported on the expression of polytopic bacterial membrane proteins (Page et al. 2006), most multiple-TM polypeptides from higher organisms have been expressed as fusion proteins followed by either enzymatic or chemical cleavage from their fusion partners. Enzymes used to release the hydrophobic membrane peptides are often deactivated by the detergents that are required to solubilize the expressed fusion proteins. Thus yields are poor and much material is wasted. Cyanogen bromide (CNBr) is usually the chosen reagent for chemical cleavage, but is incompatible with the occurrence of internal methionine residues, limiting its general usage. In this study a relatively long double-TM domain (approx. one third of the sequence of the entire receptor) from a human receptor was expressed without a fusion partner. This approach allowed expression of the wild-type protein sequence, eliminated the cleavage step, simplified purification and resulted in a final yield of 6 mg/l of culture. It should be noted that expression of entire GPCRs has been accomplished in various hosts, as fusion proteins as well as directly, and work in this area has been reviewed (Sarramegna et al. 2003, 2006).

Purity and homogeneity are critical factors affecting the quality of NMR spectra. Considering that ^{15}N-NH_4Cl is comparably cheap and that [^{15}N,^{1}H]-TROSY spectra deliver a wealth of information on the state of the protein, we decided to monitor each step of purification using ^{15}N,^{1}H-correlation spectroscopy using only ^{15}N-labeled protein. We noticed a number of interesting points: (1) The Ni-NTA affinity chromatography seemed to result in pure protein as visualized by SDS-PAGE, however the spectral quality from such samples was clearly insufficient (Fig. 3); (2) due to the presence of 6 cysteines, the protein was prone to forming aggregates that result in severe line broadening, and work-up under strongly reducing conditions was mandatory (Fig. 3); (3) the dramatic improvement after HPLC purification indicated the presence of non-proteinaceous contaminants, which cannot be readily removed by affinity chromatography. The chemical nature of the contaminants has not been identified so far,

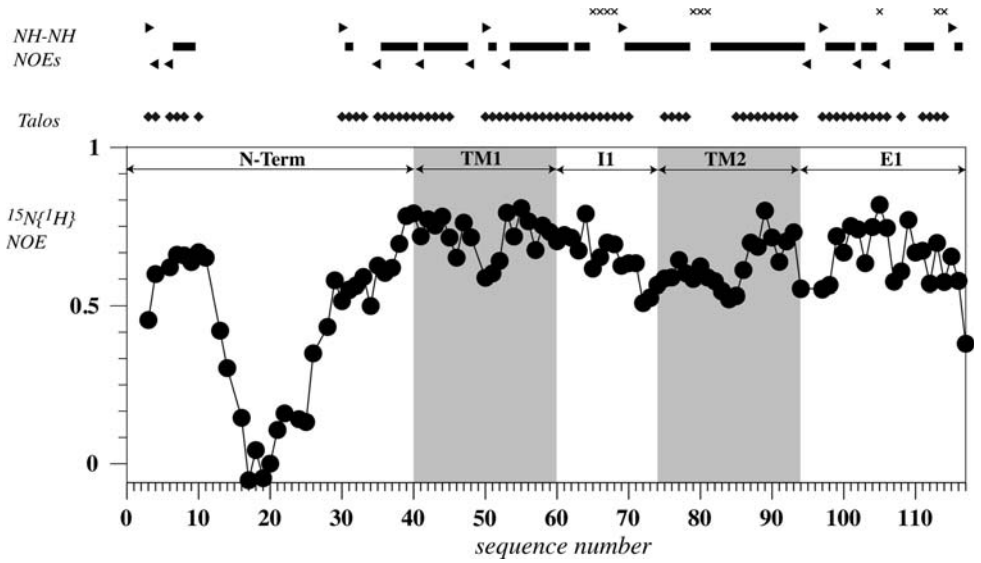

Fig. 7 Summary of the $^{15}N\{^{1}H\}$-NOE values for N-TM1-TM2 (bottom), predicted regions of helical structure based on ^{15}N,$^{13}C\alpha\beta$ and C′ chemical shifts using the program TALOS (middle) and the presence of NOEs between sequential amide protons (top). Amide moieties displaying NOEs to both preceding and following residues are indicated by squares, and by triangles with the top to the left or right for those residues that only display contact to predecessors or successor, respectively. All segments with degeneracy of proton chemical shifts that does not allow identification of NOE cross peaks are indicated by crosses

but we suspect them to be molecules that strongly associate with the protein so that they are not stripped off during the hydrophilic elution conditions of the affinity chromatography. This result suggests that they may be lipids or other hydrophobic components of the plasma membrane, that possibly also associate with the receptor in its natural environment. Another possibility is that they are proteins that bind to the metal affinity column. The presence of such contaminants apparently leads to heterogeneity in the microenvironment of the protein chains, in particular in the vicinity of the TM segments. This could affect the conformational exchange processes leading to the observed line-broadening. While HPLC purification is a standard technique for peptide chemists, it is often not used by protein biochemists because the solvent conditions denature most globular proteins. The possible presence of associating non-proteinaceous or proteinaceous contaminants is relevant to crystallographers who usually judge protein purity from SDS-PAGE gels. Perhaps screening of sample purity by ^{15}N,^{1}H NMR, at least for some of the smaller membrane proteins systems, could prove useful prior to embarking on crystallization attempts. We are aware that the proposed procedure requires a refolding step. In the context of entire GPCRs such refolding may not be achieved easily. However, in literature precedents that such refolding is possible can be found (Baneres et al. 2003, 2005; Kiefer et al. 1996).

Membrane proteins can only properly exert their function when inserted in the membrane. Natural membranes, however, are characterized by the following features: they are patchy, with segregated regions of different chemical composition, variable thickness and distinct function (Engelman 2005). To mimic this environment various media have been developed such as detergent micelles (Krüger-Koplin et al. 2004), bicelles (Glover et al. 2001; Vold et al. 1997; Poget and Girvin 2007) amphipols (Gohon et al. 2008; Zoonens et al. 2005), and very recently nanoscale bilayers (Lyukmanova et al. 2008) (for a general review on the usage of detergents in NMR studies of membrane proteins see Sanders et al. 2004; Sanders and Oxenoid 2000; Sanders and Sönnichsen 2006). For reasons of simplicity micelles have been frequently employed for NMR studies. In our study a wide range of detergents have been tested: Sarcosyl, LDAO, and DDM did not solubilize N-TM1-TM2. LPPG and LMPG only dissolved it to a very low extent, and others including DPC, OGP and DHPC dissolved the protein, but resulted in extremely broad spectra. Based on heteronuclear NOE analyses SDS resulted in a non-uniquely structured protein, an observation frequently also reported by other groups (Krüger-Koplin et al. 2004). The result of the detergent screening conducted in this study indicated that it may be useful to consider detergent mixtures when optimizing membrane protein solubility and integration into micelles. In the case of N-TM1-TM2 neither LPPG nor DPC gave satisfactory results, but the combination of these detergents resulted in a high-quality [^{15}N,^{1}H]-TROSY spectrum, in which 107 out of the expected 109 (without counting residues from the His-tag) peaks were observed. The final composition exhibited long-term stability and allowed us to run all of

the three dimensional experiments required for a structural analysis. Natural membranes are heterogeneous mixtures of a variety of lipids and proteins. We suspect that various detergents can play different roles in solubilizing the peptide, aiding its integration into the lipid-like environment and forming a relatively stable composition. In the present example the LPPG head group is likely a much better mimic of head groups of naturally occurring lipids than DPC because the central glycerol component is retained. For reasons that are unclear to us at the moment, LPPG's capability to spontaneously allow insertion of the N-TM1-TM2 protein is low and it does not solubilize the purified polypeptide. In contrast DPC micelles readily integrate the membrane protein but give extremely broad lines in the HSQC spectra, possibly reflecting the presence of conformational exchange. The ratio between DPC and LPPG was, therefore, chosen to represent the minimal amount of DPC required to dissolve the protein. The optimized composition gave a highly resolved HSQC spectrum perhaps indicating that LPPG-peptide contacts are maximized in the TM region resulting in a relatively homogeneous microenvironment that led to good spectroscopic properties. By using a combination of detergents the number of membrane mimetic environments can be greatly increased and the possibility for trials that can exploit the synergistic contributions of different head groups and hydrophobic matches is maximized. It is important to note that protein detergent complexes are not idealized micelles and the insertion of detergents with different chain lengths at various positions in an asymmetric composition might, from a thermodynamic perspective, be predicted to lead to an optimally packed protein-lipid.

Inspection of NOEs between sequential amide protons, and restraints from chemical shifts delivered by TALOS allowed the derivation of the first low-resolution picture of secondary structure in the N-TM1-TM2 polypeptide. Stretches of the putative TM helices are predominantly helical (see Fig. 7). However, in the regions proximal to polar residues in the TMs (E and D in TM1 and TM2, respectively) the helices are destabilized, as judged by the reduction in the heteronuclear NOEs, by the TALOS predictions, by enhanced amide proton exchange and by the absence of contacts between sequential amide protons. Buried glutamic acid and aspartic acid residues are rarely found in TM domains of integral membrane proteins, and we have noted such increased flexibility on another isolated TM domain in DPC micelles(Neumoin et al. 2007). The biological significance of these findings will be subject to future work. A particularly interesting finding is, that the I1 and E1 loops are predominantly helical. The sequence of the beginning of the I1 loop is amphiphilic, and may possibly form a surface-associated helix. The sequence of the E1 loop is also amphiphilic in nature. In addition, it is rich in aromatic residues that are expected to position it in the interfacial compartment. Given the strong energetic driving force to place E1 in the interface compartment it is unlikely that E1 forms a flexible loop that diffuses into bulk solution. In the published crystal structures from rhodopsin (Palczewski et al. 2000) and the β-adrenergic receptors (Rosenbaum et al. 2007; Warne et al. 2008), the long E2 loop contained elements of secondary structure; in the case of rhodopsin a short β-sheet, in the case of the β1- and β2-adrenergic receptors α-helices. However, the I1 and the E1 loops were devoid of regular secondary structure. Whether the helical nature of the E1 and I1 domains of N-TM1-TM2 is biologically relevant awaits additional studies on larger Y4 receptor fragments. At present it is also unclear how the I1 and E1 helices would connect the TM helices and reinsert smoothly into the membrane. However, in GPCR structures published to date we note that the length of the TM helices is not generally conserved—the TM5 and TM6 of squid rhodopsin were surprisingly deeply penetrating into the cytosol (Murakami and Kouyama 2008).

Previously, we reported the conformational preferences of the isolated N-terminal domain in the presence of DPC micelles (Zou et al. 2008). The comparison of the dynamics data indicate that the latter and the corresponding fragment from the N-TM1-TM2 protein are highly similar in that they contain a short helix comprising residues 5–10, followed by a long and unstructured loop between residues 11 and 30. The segment that connects that loop to the first TM (residues 31 to 40) is rather flexible in the isolated N-Y4 peptide, but mostly helical in N-TM1-TM2. The amphiphilic sequence of the N-terminal region of N-TM1-TM2 is compatible with the presence of a surface-associated helix. Such a helix was also observed by us on a similar construct from the Ste2p receptor, a family D GPCR from yeast (unpublished results).

Conclusions

To conclude we have developed a synthetic route for directly expressing and isolating double-domain mammalian GPCR fragment in isotopically-labelled form in good yield. Rigorous purification using a combination of affinity chromatography and reversed-phase HPLC resulted in a sample with dramatically altered biophysical properties. A rational method for NMR sample optimization is introduced that relies on mixtures of detergents. The methodology allowed the collection of good-quality 3D NMR spectra, and preliminary results indicated the protein to be highly structured in the LPPG/DPC mixed micelles. Future work will be aimed at fully establishing the secondary and tertiary structure of this important domain of human N-Y4. We believe that the presented methodology

may also be useful in the studies of even larger fragments or entire receptors.

Acknowledgements We would like to thank for financial support from the Swiss National Science Foundation (grant No. 3100A0-11173 to CZ), from the Alfred Werner Legat (to OZ) and from the National Institutes of Health (GM22086 to FN).

References

Baneres JL, Martin A, Hullot P, Girard JP, Rossi JC, Parello J (2003) Structure-based analysis of GPCR function: conformational adaptation of both agonist and receptor upon leukotriene B4 binding to recombinant BLT1. J Mol Biol 329:801–814

Banères JL, Mesnier D, Martin A, Joubert L, Dumuis A, Bockaert J (2005) Molecular characterization of a purified 5-HT4 receptor: a structural basis for drug efficacy. J Biol Chem 280:20253–20260

Bennett M, Yeagle JA, Maciejewski M, Ocampo J, Yeagle PL (2004) Stability of loops in the structure of lactose permease. Biochemistry 43:12829–12837

Boyd D, Schierle C, Beckwith J (1998) How many membrane proteins are there? Protein Sci 7:201–205

Cherezov V, Rosenbaum DM, Hanson MA, Rasmussen SG, Thian FS, Kobilka TS, Choi HJ, Kuhn P, Weis WI, Kobilka BK, Stevens RC (2007) High-resolution crystal structure of an engineered human beta2-adrenergic G protein-coupled receptor. Science 318:1258–1265

Cohen LS, Arshava B, Estephan R, Englander J, Kim H, Hauser M, Zerbe O, Ceruso M, Becker JM, Naider F (2008) Expression and biophysical analysis of two double-transmembrane domain-containing fragments from a yeast G protein-coupled receptor. Biopolymers 90:117–130

Cornilescu G, Delaglio F, Bax A (1999) Protein backbone angle restraints from searching a database for chemical shift and sequence homology. J Biomol NMR 13:289–302

Drew D, Froderberg L, Baars L, De Gier JW (2003) Assembly and overexpression of membrane proteins in *Escherichia coli*. Biochim Biophys Acta 1610:3–10

Drew D, Slotboom DJ, Friso G, Reda T, Genevaux P, Rapp M, Meindl-Beinker NM, Lambert W, Lerch M, Daley DO, Van Wijk KJ, Hirst J, Kunji E, De Gier JW (2005) A scalable, GFP-based pipeline for membrane protein overexpression screening and purification. Protein Sci 14:2011–2017

Engelman DM (2005) Membranes are more mosaic than fluid. Nature 438:578–580

Foord SM (2002) Receptor classification: post genome. Curr Opin Pharmacol 2:561–566

Getmanova E, Patel AB, Klein-Seetharaman J, Loewen MC, Reeves PJ, Friedman N, Sheves M, Smith SO, Khorana HG (2004) NMR spectroscopy of phosphorylated wild-type rhodopsin: mobility of the phosphorylated C-terminus of rhodopsin in the dark and upon light activation. Biochemistry 43:1126–1133

Glover KJ, Whiles JA, Wu G, Yu N, Deems R, Struppe JO, Stark RE, Komives EA, Vold RR (2001) Structural evaluation of phospholipid bicelles for solution-state studies of membrane-associated biomolecules. Biophys J 81:2163–2171

Gohon Y, Dahmane T, Ruigrok RW, Schuck P, Charvolin D, Rappaport F, Timmins P, Engelman DM, Tribet C, Popot JL, Ebel C (2008) Bacteriorhodopsin/amphipol complexes: structural and functional properties. Biophys J 94:3523–3537

Grisshammer R, White JF, Trinh LB, Shiloach J (2005) Large-scale expression and purification of a G-protein-coupled receptor for structure determination–an overview. J Struct Funct Genomics 6:159–163

Harmar AJ (2001) Family-B G-protein-coupled receptors. Genome Biol 2:30131–3013.10

Hessa T, Kim H, Bihlmaier K, Lundin C, Boekel J, Andersson H, Nilsson I, White SH, Von Heijne G (2005) Recognition of transmembrane helices by the endoplasmic reticulum translocon. Nature 433:377–381

Hessa T, Meindl-Beinker NM, Bernsel A, Kim H, Sato Y, Lerch-Bader M, Nilsson I, White SH, von Heijne G (2007) Molecular code for transmembrane-helix recognition by the Sec61 translocon. Nature 450:1026–1030

Hopkins AL, Groom CR (2002) The druggable genome. Nat Rev Drug Discov 1:727–730

Howell SC, Mesleh MF, Opella SJ (2005) NMR structure determination of a membrane protein with two transmembrane helices in micelles: MerF of the bacterial mercury detoxification system. Biochemistry 44:5196–5206

Huang KS, Bayley H, Liao MJ, London E, Khorana HG (1981) Refolding of an integral membrane protein. Denaturation, renaturation, and reconstitution of intact bacteriorhodopsin and two proteolytic fragments. J Biol Chem 256:3802–3809

Jacoby E, Bouhelal R, Gerspacher M, Seuwen K (2006) The 7 TM G-protein-coupled receptor target family. Chem Med Chem 1:761–782

Kahn TW, Engelman DM (1992) Bacteriorhodopsin can be refolded from two independently stable transmembrane helices and the complementary five-helix fragment. Biochemistry 31:6144–6151

Katragadda M, Alderfer JL, Yeagle PL (2001a) Assembly of a polytopic membrane protein structure from the solution structures of overlapping peptide fragments of bacteriorhodopsin. Biophys J 81:1029–1036

Katragadda M, Chopra A, Bennett M, Alderfer JL, Yeagle PL, Albert AD (2001b) Structures of the transmembrane helices of the G-protein coupled receptor, rhodopsin. J Pept Res 58:79–89

Kay LE, Keifer P, Saarien T (1992) Pure absorption gradient enhanced heteronuclear single-quantum correlation sepctroscopy with improved sensitivity. J Am Chem Soc 114:10663–10665

Keeler J, Clowes RT, Davis AL, Laue ED (1994) Pulsed-field gradients: theory and practice. Methods Enzymol 239:145–207

Keller R (2004) The computer aided resonance assignment. CANTINA Verlag, Goldau

Kiefer H, Krieger J, Olszewski JD, Von Heijne G, Prestwich GD, Breer H (1996) Expression of an olfactory receptor in *Escherichia coli*: purification, reconstitution, and ligand binding. Biochemistry 35:16077–16084

Klammt C, Srivastava A, Eifler N, Junge F, Beyermann M, Schwarz D, Michel H, Dötsch V, Bernhard F (2007) Functional analysis of cell-free-produced human endothelin B receptor reveals transmembrane segment 1 as an essential area for ET-1 binding and homodimer formation. FEBS J 274:3257–3269

Klein-Seetharaman J, Reeves PJ, Loewen MC, Getmanova EV, Chung J, Schwalbe H, Wright PE, Khorana HG (2002) Solution NMR spectroscopy of [alpha-^{15}N]lysine-labeled rhodopsin: The single peak observed in both conventional and TROSY-type HSQC spectra is ascribed to Lys-339 in the carboxyl-terminal peptide sequence. Proc Natl Acad Sci USA 99:3452–3457

Klein-Seetharaman J, Yanamala NV, Javeed F, Reeves PJ, Getmanova EV, Loewen MC, Schwalbe H, Khorana HG (2004) Differential dynamics in the G protein-coupled receptor rhodopsin revealed by solution NMR. Proc Natl Acad Sci USA 101:3409–3413

Krüger-Koplin RD, Sorgen PL, Krüger-Koplin ST, Rivera-Torres IO, Cahill SM, Hicks DB, Grinius L, Krulwich TA, Girvin ME (2004) An evaluation of detergents for NMR structural studies of membrane proteins. J Biomol NMR 28:43–57

Lau TL, Partridge AW, Ginsberg MH, Ulmer TS (2008) Structure of the integrin beta3 transmembrane segment in phospholipid bicelles and detergent micelles. Biochemistry 47:4008–4016

Lee BK, Jung KS, Son C, Kim H, Verberkmoes NC, Arshava B, Naider F, Becker JM (2007) Affinity purification and characterization of a G-protein coupled receptor, Saccharomyces cerevisiae Ste2p. Prot Expr Purif 56:62–71

Lyukmanova EN, Shenkarev ZO, Paramonov AS, Sobol AG, Ovchinnikova TV, Chupin VV, Kirpichnikov MP, Blommers MJ, Arseniev AS (2008) Lipid-protein nanoscale bilayers: a versatile medium for NMR investigations of membrane proteins and membrane-active peptides. J Am Chem Soc 130:2140–2141

Ma D, Liu Z, Li L, Tang P, Xu Y (2005) Structure and dynamics of the second and third transmembrane domains of human glycine receptor. Biochemistry 44:8790–8800

Mackenzie KR, Prestegard JH, Engelman DM (1997) A transmembrane helix dimer—structure and implications. Science 276:131–133

Martin NP, Leavitt LM, Sommers CM, Dumont ME (1999) Assembly of G protein-coupled receptors from fragments: identification of functional receptors with discontinuities in each of the loops connecting transmembrane segments. Biochemistry 38:682–695

Massotte D (2003) G protein-coupled receptor overexpression with the baculovirus-insect cell system: a tool for structural and functional studies. Biochim Biophys Acta 1610:77–89

Miroux B, Walker JE (1996) Over-production of proteins in *Escherichia coli*: mutant hosts that allow synthesis of some membrane proteins and globular proteins at high levels. J Mol Biol 260:289–298

Mobley CK, Myers JK, Hadziselimovic A, Ellis CD, Sanders CR (2007) Purification and initiation of structural characterization of human peripheral myelin protein 22, an integral membrane protein linked to peripheral neuropathies. Biochemistry 46:11185–11195

Murakami M, Kouyama T (2008) Crystal structure of squid rhodopsin. Nature 453:363–367

Musial-Siwek M, Kendall DA, Yeagle PL (2008) Solution NMR of signal peptidase, a membrane protein. Biochim Biophys Acta 1778:937–944

Neumoin A, Arshava B, Becker J, Zerbe O, Naider F (2007) NMR studies in dodecylphosphocholine of a fragment containing the seventh transmembrane helix of a G-protein-coupled receptor from Saccharomyces cerevisiae. Biophys J 93:467–482

Noggle JH, Schirmer RE (1971) The nuclear overhauser effect—chemical applications. Academic Press, New York

O'Hara PJ, Sheppard PO, Thogersen H, Venezia D, Haldeman BA, Mcgrane V, Houamed KM, Thomsen C, Gilbert TL, Mulvihill ER (1993) The ligand-binding domain in metabotropic glutamate receptors is related to bacterial periplasmic binding proteins. Neuron 11:41–52

Oxenoid K, Kim HJ, Jacob J, Sonnichsen FD, Sanders CR (2004) NMR assignments for a helical 40 kDa membrane protein. J Am Chem Soc 126:5048–5049

Page RC, Moore JD, Nguyen HB, Sharma M, Chase R, Gao FP, Mobley CK, Sanders CR, Ma L, Sönnichsen FD, Lee S, Howell SC, Opella SJ, Cross TA (2006) Comprehensive evaluation of solution nuclear magnetic resonance spectroscopy sample preparation for helical integral membrane proteins. J Struct Func Genom 7:51–64

Palczewski K, Kumasaka T, Hori T, Behnke CA, Motoshima H, Fox BA, Le Trong I, Teller DC, Okada T, Stenkamp RE, Yamamoto M, Miyano M (2000) Crystal structure of rhodopsin: a G protein-coupled receptor. Science 289:739–745

Park JH, Scheerer P, Hofmann KP, Choe HW, Ernst OP (2008) Crystal structure of the ligand-free G-protein-coupled receptor opsin. Nature 454:183–187

Pervushin K, Riek R, Wider G, Wüthrich K (1997) Attenuated T2 relaxation by mutual cancellation of dipole-dipole coupling and chemical shift anisotropy indicates an avenue to NMR structures of very large biological macromolecules in solution. Proc Natl Acad Sci USA 94:12366–12371

Poget SF, Girvin ME (2007) Solution NMR of membrane proteins in bilayer mimics: small is beautiful, but sometimes bigger is better. Biochim Biophys Acta 1768:3098–3106

Popot JL, Engelman DM (1990) Membrane protein folding and oligomerization: the two-stage model. Biochemistry 29:4031–4037

Popot JL, Engelman DM (2000) Helical membrane protein folding, stability, and evolution. Annu Rev Biochem 69:881–922

Rastogi VK, Girvin ME (1999) Structural changes linked to proton translocation by subunit c of the ATP synthase. Nature 402:263–268

Ridge KD, Lee SS, Yao LL (1995) In vivo assembly of rhodopsin from expressed polypeptide fragments. Proc Natl Acad Sci USA 92:3204–3208

Rosenbaum DM, Cherezov V, Hanson MA, Rasmussen SG, Thian FS, Kobilka TS, Choi HJ, Yao XJ, Weis WI, Stevens RC, Kobilka BK (2007) GPCR engineering yields high-resolution structural insights into beta2-adrenergic receptor function. Science 318:1266–1273

Salzmann M, Pervushin K, Wider G, Senn H, Wüthrich K (1998) TROSY in triple-resonance experiments: new perspectives for sequential NMR assignment of large proteins. Proc Natl Acad Sci USA 95:13585–13590

Salzmann M, Wider G, Pervushin K, Senn H, Wüthrich K (1999) TROSY-type triple-resonance experiments for sequential NMR assignments of large proteins. J Am Chem Soc 121:844–848

Sanders CR, Oxenoid K (2000) Customizing model membranes and samples for NMR spectroscopic studies of complex membrane proteins. Biochim Biophys Acta 1508:129–145

Sanders CR, Sönnichsen F (2006) Solution NMR of membrane proteins: practice and challenges. Magn Reson Chem 44:S24–S40

Sanders C, Kuhn Hoffmann A, Gray D, Keyes M, Ellis CD (2004) French swimwear for membrane proteins. ChemBioChem 5:423–426

Sarramegna V, Talmont F, Demange P, Milon A (2003) Heterologous expression of G-protein-coupled receptors: comparison of expression systems fron the standpoint of large-scale production and purification. Cell Mol Life Sci 60:1529–1546

Sarramegn V, Muller I, Milon A, Talmont F (2006) Recombinant G protein-coupled receptors from expression to renaturation: a challenge towards structure. Cell Mol Life Sci 63:1149–1164

Schubert M, Kolbe M, Kessler B, Oesterhelt D, Schmieder P (2002) Heteronuclear multidimensional NMR spectroscopy of solubilized membrane proteins: resonance assignment of native bacteriorhodopsin. ChemBioChem 3:1019–1023

Shan X, Gardner K, Muhandiram D, Rao NS, Arrowsmith C, Kay LE (1996) Assignment of N-15, C-13(alpha), C-13(beta), and HN resonances in an N-15, C-13, H-2 labeled 64 kDa trp repressor-operator complex using triple-resonance NMR spectroscopy and H-2-decoupling. J Am Chem Soc 118:6570–6579

Stevens TJ, Arkin IT (2000) Do more complex organisms have a greater proportion of membrane proteins in their genomes? Proteins 39:417–420

Tian C, Breyer RM, Kim HJ, Karra MD, Friedman DB, Karpay A, Sanders CR (2005) Solution NMR spectroscopy of the human vasopressin V2 receptor, a G protein-coupled receptor. J Am Chem Soc 127:8010–8011

Tian C, Vanoye CG, Kang C, Welch RC, Kim HJ, George AL, Sanders CR (2007) Preparation, functional characterization, and NMR studies of human KCNE1, a voltage-gated potassium

channel accessory subunit associated with deafness and long QT syndrome. Biochemistry 46:11459–11472

Venter JC, Adams MD, Myers EW, Li PW, Mural RJ, Sutton GG, Smith HO, Yandell M, Evans CA, Holt RA, Gocayne JD, Amanatides P, Ballew RM, Huson DH, Wortman JR, Zhang Q, Kodira CD, Zheng XH, Chen L, Skupski M, Subramanian G, Thomas PD, Zhang J, Gabor Miklos GL, Nelson C, Broder S, Clark AG, Nadeau J, Mckusick VA, Zinder N, Levine AJ, Roberts RJ, Simon M, Slayman C, Hunkapiller M, Bolanos R, Delcher A, Dew I, Fasulo D, Flanigan M, Florea L, Halpern A, Hannenhalli S, Kravitz S, Levy S, Mobarry C, Reinert K, Remington K, Abu-Threideh J, Beasley E, Biddick K, Bonazzi V, Brandon R, Cargill M, Chandramouliswaran I, Charlab R, Chaturvedi K, Deng Z, Di Francesco V, Dunn P, Eilbeck K, Evangelista C, Gabrielian AE, Gan W, Ge W, Gong F, Gu Z, Guan P, Heiman TJ, Higgins ME, Ji RR, Ke Z, Ketchum KA, Lai Z, Lei Y, Li Z, Li J, Liang Y, Lin X, Lu F, Merkulov GV, Milshina N, Moore HM, Naik AK, Narayan VA, Neelam B, Nusskern D, Rusch DB, Salzberg S, Shao W, Shue B, Sun J, Wang Z, Wang A, Wang X, Wang J, Wei M, Wides R, Xiao C, Yan C, Yao A, Ye J, Zhan M, Zhang W, Zhang H, Zhao Q, Zheng L, Zhong F, Zhong W, Zhu S, Zhao S, Gilbert D, Baumhueter S, Spier G, Carter C, Cravchik A, Woodage T, Ali F, An H, Awe A, Baldwin D, Baden H, Barnstead M, Barrow I, Beeson K, Busam D, Carver A, Center A, Cheng ML, Curry L, Danaher S, Davenport L, Desilets R, Dietz S, Dodson K, Doup L, Ferriera S, Garg N, Gluecksmann A, Hart B, Haynes J, Haynes C, Heiner C, Hladun S, Hostin D, Houck J, Howland T, Ibegwam C, Johnson J, Kalush F, Kline L, Koduru S, Love A, Mann F, May D, Mccawley S, Mcintosh T, Mcmullen I, Moy M, Moy L, Murphy B, Nelson K, Pfannkoch C, Pratts E, Puri V, Qureshi H, Reardon M, Rodriguez R, Rogers YH, Romblad D, Ruhfel B, Scott R, Sitter C, Smallwood M, Stewart E, Strong R, Suh E, Thomas R, Tint NN, Tse S, Vech C, Wang G, Wetter J, Williams S, Williams M, Windsor S, Winn-Deen E, Wolfe K, Zaveri J, Zaveri K, Abril JF, Guigo R, Campbell MJ, Sjolander KV, Karlak B, Kejariwal A, Mi H, Lazareva B, Hatton T, Narechania A, Diemer K, Muruganujan A, Guo N, Sato S, Bafna V, Istrail S, Lippert R, Schwartz R, Walenz B, Yooseph S, Allen D, Basu A, Baxendale J, Blick L, Caminha M, Carnes-Stine J, Caulk P, Chiang YH, Coyne M, Dahlke C, Mays A, Dombroski M, Donnelly M, Ely D, Esparham S, Fosler C, Gire H, Glanowski S, Glasser K, Glodek A, Gorokhov M, Graham K, Gropman B, Harris M, Heil J, Henderson S, Hoover J, Jennings D, Jordan C, Jordan J, Kasha J, Kagan L, Kraft C, Levitsky A, Lewis M, Liu X, Lopez J, Ma D, Majoros W, Mcdaniel J, Murphy S, Newman M, Nguyen T, Nguyen N, Nodell M, Pan S, Peck J, Peterson M, Rowe W, Sanders R, Scott J, Simpson M, Smith T, Sprague A, Stockwell T, Turner R, Venter E, Wang M, Wen M, Wu D, Wu M, Xia A, Zandieh A, Zhu X (2001) The sequence of the human genome. Science 291: 1304–1351

Vold RR, Prosser RS, Deese AJ (1997) Isotropic solutions of phospholipid bicelles—a new membrane mimetic for high-resolution NMR studies of polypeptides. J Biomol NMR 9:329–335

Warne T, Serrano-Vega MJ, Baker J, Moukhametzianov R, Edwards P, Henderson R, Leslie A, Tate C, Schertler G (2008) Structure of a beta1-adrenergic G-protein-coupled receptor. Nature 454:486–491

Wedekind A, O'malley MA, Niebauer RT, Robinson AS (2006) Optimization of the human adenosine A2a receptor yields in Saccharomyces cerevisiae. Biotechnol Prog 22:1249–1255

Weigelt J (1998) Single scan, sensitivity- and gradient-enhanced TROSY for multidimensional NMR experiments. J Am Chem Soc 120:10778–10779

Werner K, Richter C, Klein-Seetharaman J, Schwalbe H (2008) Isotope labeling of mammalian GPCRs in HEK293 cells and characterization of the C-terminus of bovine rhodopsin by high resolution liquid NMR spectroscopy. J Biomol NMR 40:49–53

White SH, Wimley WC (1999) Membrane protein folding and stability: physical principles. Annu Rev Biophys Biomol Struct 28:319–365

Wishart DS, Sykes BD (1994) The 13C chemical-shift index: a simple method for the identification of protein secondary structure using ^{13}C chemical-shift data. J Biomol NMR 4:171–180

Wishart D, Sykes B, Richards F (1991) Relationship between nuclear magnetic resonance chemical shift and protein secondary structure. J Mol Biol 222:311–333

Wittekind M, Mueller L (1993) HNCACB, a high-sensitivity 3D NMR experiment to correlate amide-proton and nitrogen resonances with the alpha-carbon and beta-carbon resonances in proteins. J Magn Reson Ser B 101:201–205

Wrubel W, Stochaj U, Ehring R (1994) Construction and in vivo analysis of new split lactose permeases. FEBS Lett 349:433–438

Yamazaki T, Lee W, Arrowsmith C, Muhandiram D, Kay LE (1994) A suite of triple-resonance NMR experiments for the backbone assignment of N-15, C-13, H2-labeled proteins with high sensitivity. J Am Chem Soc 116:11655–11666

Yeagle PL, Salloum A, Chopra A, Bhawsar N, Ali L, Kuzmanovski G, Alderfer JL, Albert AD (2000) Structures of the intradiskal loops and amino terminus of the G-protein receptor, rhodopsin. J Pept Res 55:455–465

Yin D, Gavi S, Shumay E, Duell K, Konopka JB, Malbon CC, Wang HY (2005) Successful expression of a functional yeast G-protein-coupled receptor (Ste2) in mammalian cells. Biochem Biophys Res Commun 329:281–287

Zheng H, Zhao J, Sheng W, Xie XQ (2006) A transmembrane helix-bundle from G-protein coupled receptor CB2: biosynthesis, purification, and NMR characterization. Biopolymers 83:46–61

Zoonens M, Catoire LJ, Giusti F, Popot JL (2005) NMR study of a membrane protein in detergent-free aqueous solution. Proc Natl Acad Sci USA 102:8893–8898

Zou C, Kumaran S, Markovic S, Walser R, Zerbe O (2008) Studies of the structure of the N-terminal domain from the Y4 receptor, a G-protein coupled receptor, and its interaction with hormones from the NPY family. ChemBioChem 9:2276–2284